ON THE WAY TO QGP VIA J/ψ SUPPRESSION*

Claudie Gerschel

Institut de Physique Nucléaire, 91406 Orsay Cedex, France

(Received October 13, 1999)

The suppression of J/ψ production, proposed as a possible signature of the formation of a Quark–Gluon Plasma in heavy ion collisions, is reviewed in these lectures both experimentally and theoretically. A special emphasis is put on the recent results obtained by the NA50 collaboration at CERN in Pb–Pb collisions where new features seem to appear.

PACS numbers: 12.38.Mh, 25.75.–q, 25.75.Dw

1. Introduction

In 1986, Matsui and Satz proposed that the suppression of charmonium state production in heavy ion collisions could be a signature of the formation of deconfined matter, the so-called Quark–Gluon Plasma (QGP) [1]. Since that time, the subject has been widely investigated both experimentally at CERN and theoretically. In these lectures, the most recent results obtained by the NA50 collaboration with the Pb beams of 158 GeV/nucleon are presented and discussed with the knowledge of the new theoretical developments in the field. The lectures are organized as follows. The first chapter is devoted to the NA50 measurements in Pb–Pb collisions as performed at CERN in 1995, 1996 and 1998. It focuses mainly on J/ψ suppression. In order to understand the physics issues, it is important to have a reference provided by hadron-induced collisions. They are discussed in a second section. Finally, in the third chapter the heavy ion results are compared to the empirical systematics deduced from p–A collisions and discussed with a particular emphasis on the most recent ideas. For more details, the reader can refer to recent overviews in Refs. [2–4].

* Presented at the XXXIX Cracow School of Theoretical Physics, Zakopane, Poland, May 29–June 8, 1999.

2. Charmonium production in Pb–Pb collisions from the NA50 experiment

2.1. Why charmonium suppression?

Charmonium states are bound states of a charm–anticharm $c\bar{c}$ pair with quantum numbers $n^{2S+1}L_J$, where n is the radial quantum number, and S, L and J denote spin, orbital and total angular momentum, respectively: $J/\psi(1^3S_1)$, $\chi_{cJ}(1^3P_J)$ with $J = 0, 1, 2$ and $\psi'(2^3S_1)$. The J/ψ and ψ' can be detected through their decay channel into a muon pair. In Reference [1], it has been suggested that, if a QGP is formed in a heavy ion collision, because of the high density of color charges in this deconfined matter, the binding potential of the c$\bar{c}$ pair is screened (Debye screening) and the bound states is no longer formed. The screening is even easier for the χ and ψ' mesons which have larger radii than J/ψ.

Two strategies are possible to search for an anomalous behaviour of the meson production rates: *i)* study different systems of target and projectiles and compare the meson cross sections in ion- and p- induced collisions or *ii)* study the meson suppression in a given heavy ion system as a function of the energy density of the collision, *i.e.* as a function of its centrality. In the latter case, a reference is needed. For the NA50 experiment which detects dimuons, this reference is provided by the well-known Drell–Yan mechanism which has the advantage of being insensitive to strong interactions and is not perturbed by the evolution of the system after hadronisation. Another reference has also been used by NA50 as explained in Section 2.3.2.

2.2. The NA50 experiment

2.2.1. Apparatus

The experimental setup is made of a muon spectrometer, detectors measuring the centrality of the collision and of an active target which allows a precise determination of the vertex of the collision and, to some extent, a rejection of the reinteraction of spectator fragments.

The spectrometer has been described in many papers (see for instance [5]). It measures dimuons in the rapidity range $0 < y_{cms} < 1$. The J/ψ mass resolution is 3.1% (r.m.s) and the acceptance for muon pairs with an invariant mass above 3 GeV/c^2 is of the order of 15%.

The vertex of the interaction is recognized with the help of an “active” target [7]. The Pb target is segmented into 7 subtargets each followed by two quartz blades located off the beam axis. While these blades allow a precise determination of the vertex, the efficiency for detecting the reinteraction of a spectator fragment is not very high. In order to evaluate the influence of the remaining reinteractions, in the 1998 experiment, only one subtarget, 3 mm thick, has been used [8] as opposed to the 7 subtargets, with a total thickness of 7 mm for 1995 [5] and 12 mm for the 1996 experiment [6].

There are 3 different centrality detectors: *i)* A Pb-fiber electromagnetic calorimeter measures the neutral transverse energy E_{T} of the particles produced in the pseudo-rapidity domain [1.1-2.3]. It is located outside the acceptance of the spectrometer in order to improve the mass resolution of the muon pairs. *ii)* A "zero-degree" calorimeter (ZDC) measures the energy E_{ZDC} carried out by the beam spectators [9]. It is based on the quartz fiber technique with a W radiator. Its angular acceptance is defined by a 60 cm long copper collimator which minimizes the contamination arising from particles produced in the collision. Its energy resolution is 7% for incident Pb nuclei. *iii)* A multiplicity detector consisting of two identical planes, with about 7000 silicon microstrips each, measures the particles in the pseudo rapidity range [1.5–3.9]. It is not used in the results presented here.

Finally, it is possible to make an off-line rejection of "unclean" events thanks to different detectors which are preinteraction and halo detectors and a segmented beam hodoscope which recognizes pile-up events.

The lay-out of the various elements of the NA50 detector in the target area is shown in Fig. 1. It can be noted in the figure that, inside the acceptance of the spectrometer, there is also a BeO preabsorber which reduces the combinatorial background due to pion and kaon decays into muon pairs to a reasonable level without spoiling the mass resolution of the spectrometer.

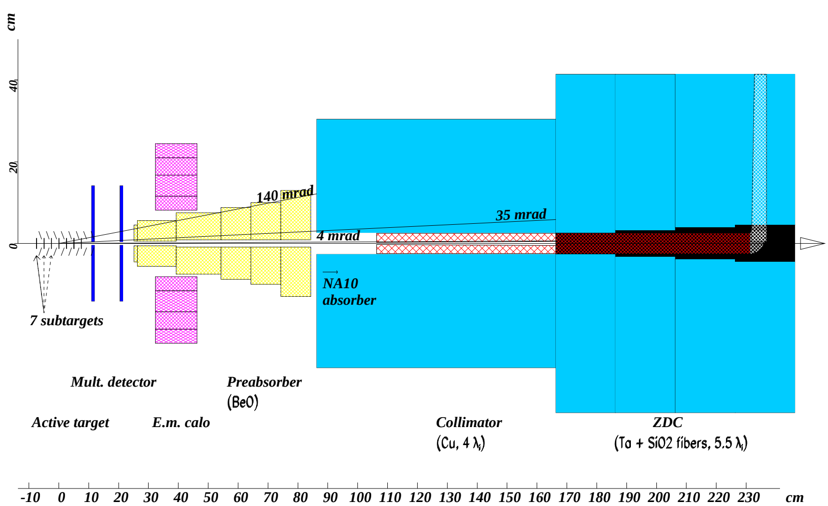

Fig. 1. Lay-out of the different elements in the target area of the NA50 detector.

2.2.2. Target identification

The active target algorithm makes use of the signal given by the two quartz blades which measure a fraction of the particles produced in the collision. When the collision is peripheral, this number decreases strongly and induces a loss of efficiency in the target identification. In order to recover a part of the peripheral events, another selection method has been developed. It is based on the correlation $E_{\rm T} - E_{\rm ZDC}$ on an event by event basis. After having applied the normal selection criteria, an additional rejection is applied to events which are outside a 2σ distance from the average correlation. This method requires a precise subtraction of events produced outside of the target, mainly on air, which are determined from "empty" target measurements. These events are non negligible only below $E_{\rm T} \simeq 30$ GeV. Figure 2 shows the number of events recovered for peripheral collisions [6].

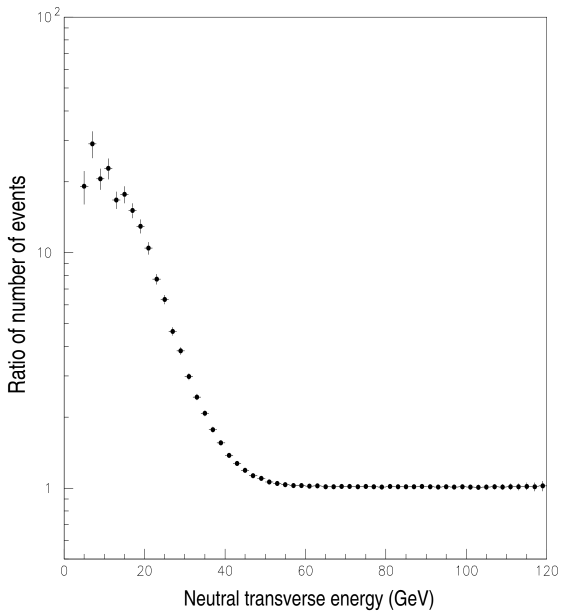

Fig. 2. Ratio of the number of events selected by the contour-cut method and by the target algorithm.

2.2.3. Trigger

Besides the usual dimuon trigger used by NA50 and previously by NA38, in each burst of the beam, there is a prescaled fraction of "minimum bias" (MB) triggers, defined by an incident ion which has interacted in the Pb target. The MB trigger fires when both the ZDC and the electromagnetic calorimeter have detected a minimum energy. This trigger provides a new reference for the study of J/ψ suppression and will be discussed further on.

2.3. Results

A typical mass spectrum is shown in Fig. 3 [6]. It is a superposition of five contributions, *i.e.* J/ψ , ψ' , Drell–Yan, open charm and the combinatorial background. The spectrum is fitted following a procedure described in Ref. [6].

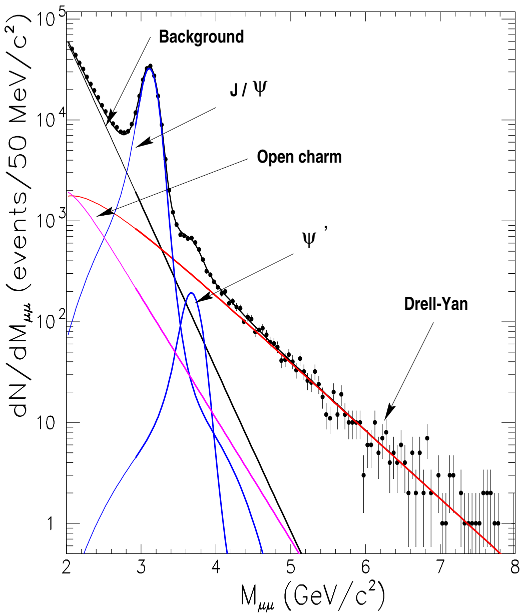

Fig. 3. Invariant mass spectrum of the opposite sign muon pairs for Pb–Pb collisions.

2.3.1. J/ψ suppression using Drell–Yan as a reference

J/ψ production is compared to that of Drell–Yan pairs in the mass range [2.9–4.5] GeV/c^2. In the following, the results labelled "1995 data" were obtained with the 7 mm segmented target. The "1996 data" provide a high statistic sample with the 12 mm segmented target and the "1998 data" give preliminary results obtained with the 3 mm single target[1]. The 1996 data

[1] For the moment, the 1998 data have been analyzed only at high E_{T} in order to study the effect of reinteractions. The low E_{T} part requires further work, in particular a careful subtraction of interactions of Pb ions with air which are relatively more important for this thinner target.

are shown in Fig. 4 for 15 centrality bins defined by E_T. There is a strong increase of J/ψ suppression between peripheral and central collisions, *i.e.* a factor of the order of 2.5.

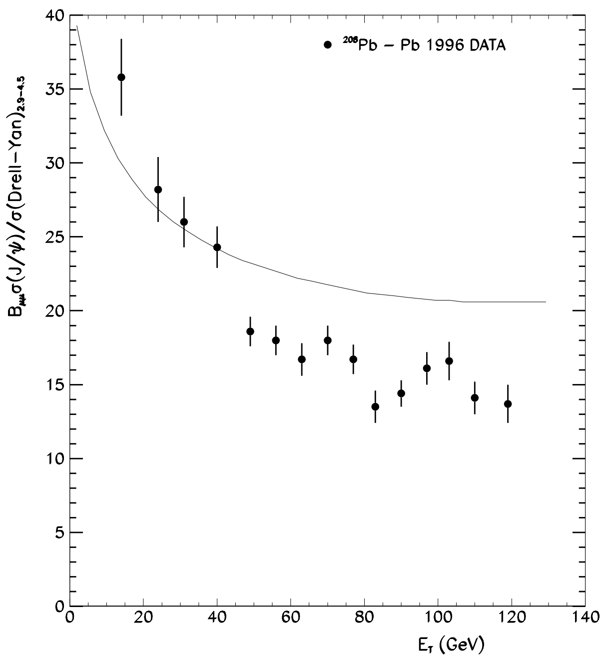

Fig. 4. J/ψ suppression using Drell–Yan as a reference. The curve represents the "normal" nuclear absorption deduced from the data obtained for lighter systems (see Section 3.2).

In order to search for the possible influence of remaining reinteractions, results obtained with the three different targets are compared in Fig. 5. Because of the low statistics of the 1995 and 1998 data, there are only 5 centrality bins. As expected [6], around $E_T = 110$ GeV, the suppression is sensitive to the thickness of the target while it is not so at lower E_T values [8].

2.3.2. J/ψ suppression using the minimum-bias events as a reference

The precision of the J/ψ suppression measurement is limited by the small statistics of the Drell–Yan events and another method has been developed which significantly reduces the statistical fluctuations [6]. The principle of this method is to obtain a "theoretical" Drell–Yan sample $N^*_{\rm DY}(E_T)$ from the statistically precise minimum bias $N^{\rm exp}_{\rm MB}(E_T)$ corresponding value.

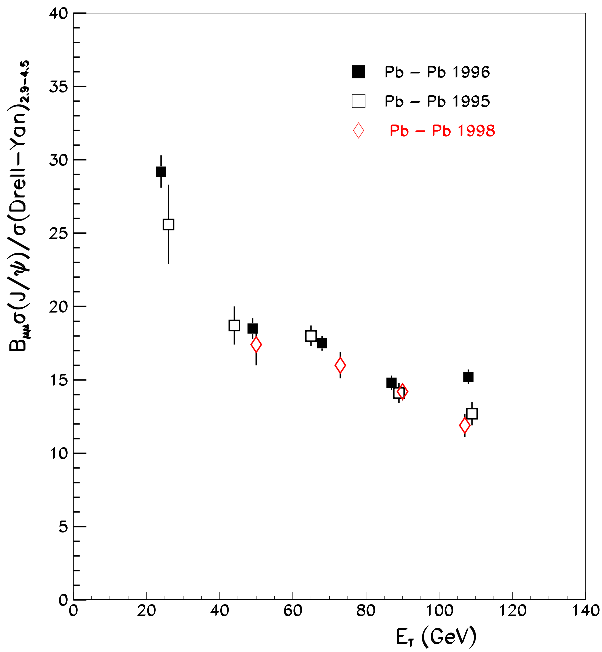

Fig. 5. J/ψ suppression using Drell–Yan as a reference for 3 different thicknesses of the Pb target.

The experimental minimum bias distribution is fitted to the expression

$$\left(\frac{dN}{dE_{\mathrm{T}}}\right)^{\mathrm{th}}_{\mathrm{MB}} \propto \int P(E_{\mathrm{T}}, b)\ b\ db\,, \tag{2.1}$$

where $P(E_{\mathrm{T}}, b)$ is the probability that a given E_{T} is measured for a collision with an impact parameter b. The analytical expression $P(E_{\mathrm{T}}, b)$ depends on two parameters E_0 and W which describe respectively the general scale of the E_{T} spectrum and the spread in E_{T} at a given impact parameter. This spread takes into account both the physical fluctuations of the number of emitted particles and the experimental fluctuations due to the limited number of particles which are measured. In particular, this spread is responsible for the slope of the high E_{T} part of the E_{T} distribution above the knee. The two parameters E_0 and W are deduced from the fit of the minimum bias distribution. In the same way, the Drell–Yan spectrum can be fitted to the relation

$$\left(\frac{dN}{dE_{\mathrm{T}}}\right)^{\mathrm{DY}}_{\mathrm{MB}} \propto \int N_{AB}(b)\ P(E_{\mathrm{T}}, b)\ b\ db\,, \tag{2.2}$$

where $N_{AB}(b)$ is the number of nucleon–nucleon collisions. It has been checked that the parameters E_0 and W obtained from this fit are similar to those obtained from the fit of the minimum bias distribution within the errors. Instead of using the experimental Drell–Yan distribution, a "theoretical" one, $(dN/dE_{\mathrm{T}})^*_{\mathrm{DY}}$, is used which is built from the minimum bias spectrum according to:

$$\left(\frac{dN}{dE}_{\mathrm{T}}\right)^*_{\mathrm{DY}} = C\left(\frac{dN}{dE}_{\mathrm{T}}\right)^{\mathrm{exp}}_{\mathrm{MB}} \; \Theta(E_{\mathrm{T}})\,, \tag{2.3}$$

where

$$\Theta(E_{\mathrm{T}}) = \frac{\left(\frac{dN}{dE}_{\mathrm{T}}\right)^{\mathrm{th}}_{\mathrm{DY}}}{\left(\frac{dN}{dE}_{\mathrm{T}}\right)^{\mathrm{th}}_{\mathrm{MB}}} \tag{2.4}$$

and C is a normalization constant. The theoretical function $\Theta(E_{\mathrm{T}})$ is plotted in Fig. 6 together with the number $N_{AB}(b)$ of nucleon–nucleon collisions evaluated from the Glauber model. The two values are similar except above the knee of the E_{T} distribution. Fig. 7 shows the comparison between the two analyses after an adjustement of the data in the region of intermediate collisions. There is a good overall agreement of the data with much smaller errors for the minimum bias reference and this analysis shows that the fluctuations of the $\psi/\mathrm{DY}^{\mathrm{exp}}$ ratio are mainly due to Drell–Yan. The minimum bias analysis is limited to values above 26 GeV because of the contribution of events produced outside of the target. This contamination is larger for minimum bias events than for the dimuon triggers. It can be noticed that, as in the case of the Drell–Yan reference, the ratio ψ/DY^* is free from most inefficiencies. However, there may be potential new systematic effects due to the use of the new trigger. The effect of the target thickness has been checked also with the minimum bias analysis (Fig. 8). The effect of unrecognized reinteractions is clearly seen on the higher part of the E_{T}-dependence [8]. Taking this effect into account, a combination of the different NA50 results, in the regions where they are unbiased, is displayed in Fig. 9. Two important features become visible: *i)* There is a strong departure, around $E_{\mathrm{T}} = 40$ GeV, from the absorption curve deduced from the data collected with lighter projectiles (see Section 3.2). *ii)* There is a second drop at high E_{T} in the suppression pattern.

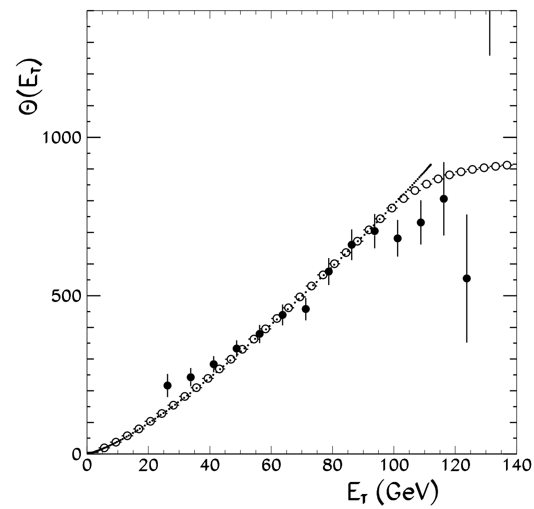

Fig. 6. Ratio of Drell–Yan to minimum bias theoretical distributions vs $E_{\rm T}$ (open circles). The corresponding experimental ratio is also shown (closed circles). Finally, the dotted line is the calculated number of nucleon–nucleon collisions.

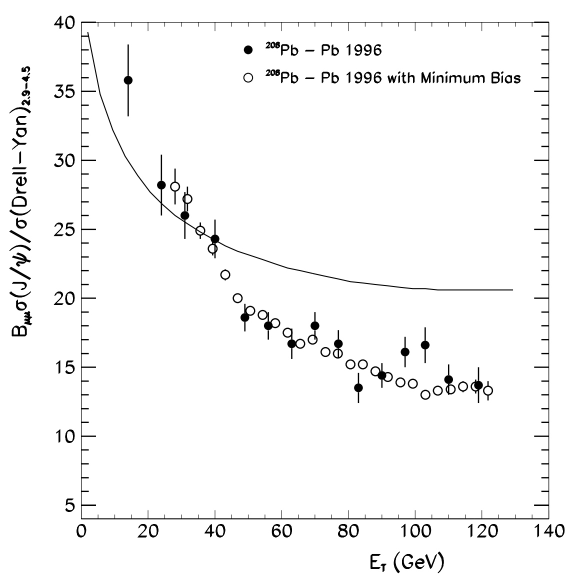

Fig. 7. Comparison of J/ψ suppression pattern using experimental or "theoretical" (from minimum bias) Drell–Yan as a reference for 1996 data. The solid line has the same meaning as for Fig. 4.

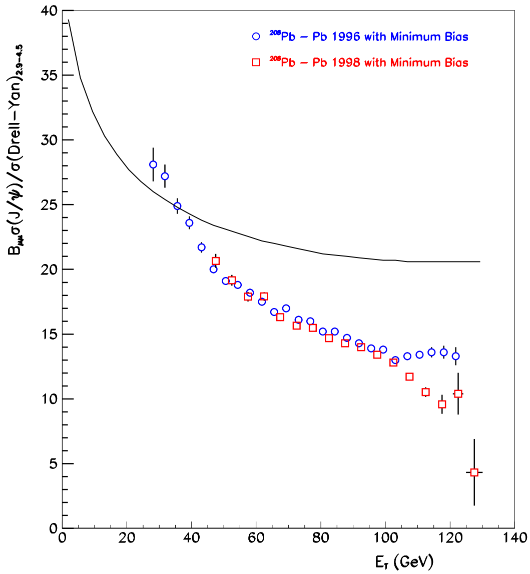

Fig. 8. Comparison of the suppression patterns between the 3 mm thick target and the 12 mm one. The reference here is the "theoretical" Drell–Yan .

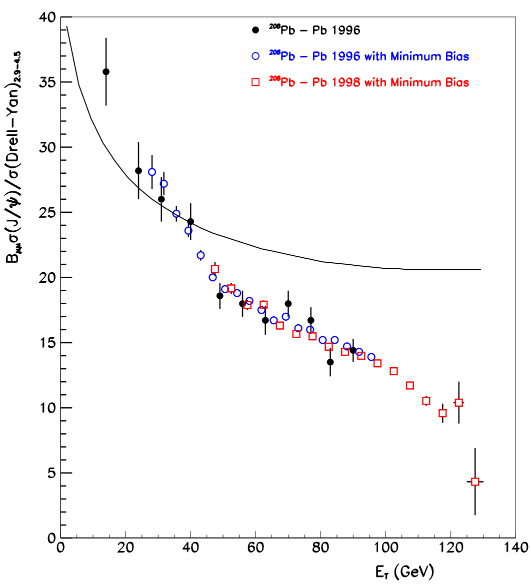

Fig. 9. Summary plot of the J/ψ suppression pattern vs E_{T} in Pb–Pb collisions. The solid line has the same meaning as for Fig. 4.

2.3.3. ψ' suppression pattern

Here we recall the main observations concerning the ψ' suppression. While the ψ' suppression is similar to that of J/ψ in p–A collisions [10, 11], ψ' is much more suppressed than J/ψ in Pb–Pb collisions [12]. The ratio $\sigma_{\psi'}/\sigma_{\mathrm{DY}}$ decreases by a factor 10 between the two extreme centrality bins.

3. p–A collisions

In order to have an experimental reference for the study of J/ψ suppression, p–A collisions have been extensively studied by different experiments for different beam energies (see for instance the review in Ref. [4]).

3.1. Empirical systematics

J/ψ suppression in p–A collisions is defined as

$$S^{A}_{J/\psi}(x_{\mathrm{F}},p_{\mathrm{T}};E_p)=\frac{d^3\sigma^{pA\to J/\psi X}/dx_{\mathrm{F}}d^2p_{\mathrm{T}}}{A\ d^3\sigma^{pN\to J/\psi X}/dx_{\mathrm{F}}d^2p_{\mathrm{T}}} \tag{3.1}$$

which relates the nuclear production cross section to the nucleon one. There are two different empirical ways to parametrize J/ψ suppression as a function of the mass number of the target which are

$$S^{A}_{J/\psi}(x_{\mathrm{F}},p_{\mathrm{T}};E_p)=A^{\alpha_\psi-1} \tag{3.2}$$

or equivalently

$$S^{A}_{J/\psi}(x_{\mathrm{F}},p_{\mathrm{T}};E_p)=\exp(-\rho_0\sigma_{\mathrm{abs}}L)\ [13] \tag{3.3}$$

where L is the mean length of nuclear matter traversed by the $c\bar{c}$ pair and ρ_0 is the normal nuclear matter density. σ_{abs} is the absorption cross section measured in an experiment where a J/ψ is detected but is not necessarily the absorption cross section of the final J/ψ itself. The x_{F}, p_{T} and beam energy dependences are contained in the parameter α or σ_{abs}. This has been widely discussed and up to very recently, the available data from NA3 [14], NA38 [11, 15], NA51 [10], E772 [16] and E789 [17] experiments, recorded in different x_{F} domains and at different beam energies between 200 and 800 GeV, gave values of α, or equivalently of σ_{abs}, which were compatible and led to a suppression coefficient $1-\alpha\simeq 0.08$ [4] or to $\sigma_{\mathrm{abs}}\simeq 6$ mb. It was thus considered that the suppression was independent of both x_{F} (for $x_{\mathrm{F}}<0.4$) and $\sqrt{s}$. New results from the E866 Fermilab experiment at 800 GeV [18] seem to contradict this assumption. Indeed, in Fig. 10, which gives values integrated over p_{T}, the α value of J/ψ remains constant in the

$x_{\rm F}$ domain [-0.05,+0.25] but closer to 1 than previously thought: $1-\alpha \simeq 0.05$ or $\sigma_{\rm abs} \simeq 3$ mb [2]. It is thus a smaller object which is absorbed. As far as

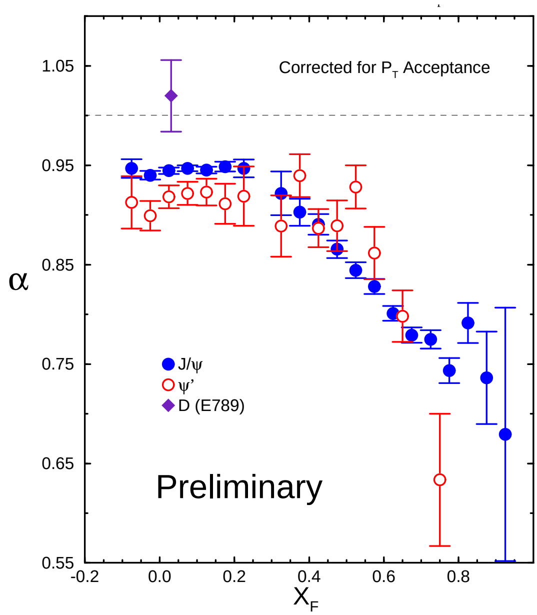

Fig. 10. Dependence of the α parameter vs $x_{\rm F}$ for J/ψ and ψ' measured by the E866 experiment [18]. The values are integrated over $p_{\rm T}$.

ψ' is concerned, up to now, its suppression was considered to be similar to that of J/ψ [10, 11, 16, 19]. With the new E866 results of Fig. 10, it can be seen that it is true only above $x_{\rm F}$=0.25. Below this value, ψ' is suppressed more strongly than J/ψ .

3.2. Nuclear absorption models

Collisions induced by hadrons have been extensively discussed in order to provide a theoretical basis for the behaviour of J/ψ in "normal" nuclear matter. Details can be found in the review paper of Ref. [4]. The main ideas only are summarized here. Today, it is considered that J/ψ suppression is not due to the absorption of the final resonances but rather of the nascent $c\bar{c}$ pair in a premeson state. The J/ψ (ψ') formation is usually described as a three-step process $gg \to [c\bar{c}]_8 \to [c\bar{c}]_1 + g \to J/\psi + g$. Two gluons fuse and a third one is radiated off in order to recover a color neutral object. The subscripts '1' or '8' refer to the singlet or octet nature of the $c\bar{c}$ pair.

[2] The difference with the larger $1-\alpha$ previous values of E772 and E789 is explained [18] by the narrow $p_{\rm T}$ window of these experiments.

The time scales of the three steps are called respectively τ_0, τ_g and τ_f. The relative value of $\gamma\tau$, where γ is the Lorentz factor, as compared to the radius R of the nucleus defines the nature of the object which traverses the matter. The time τ_0 for the first step is given by $1/2m_{\rm c}$ and is fast. Two different assumptions about the value of τ_g are considered in the following models.

- If τ_g is small enough, $\gamma\tau_g \ll R$ and a color neutral premeson traverses the nucleus. In the quantum mechanical approach of Ref. [20,21], the color singlet wave function is expanded into a set of charmonium states. In this context, it is meaningless to speak about J/ψ or ψ' before a time given by
$$\tau_f = (M_{\psi'} - M_{J/\psi})^{-1} = 0.3 \text{ fm}/c\,. \tag{3.4}$$

- If the third gluon is assumed to be soft, $\gamma\tau_g \gg R$ and a colored premeson traverses nuclear matter. Inspired by the color octet model [22,23], the model in Ref. [24] describes the premeson as made of a color octet $c\bar{c}$ pair dressed with an additional gluon, the whole being color neutral. This premeson is then a higher Fock state of the J/ψ or ψ' wave function. The gluon is radiated or absorbed outside of nuclear matter. An absorption cross section of 6–7 mb is given for the premeson.

Following the model in Ref. [24], it has been stated [25] that when the γ factor decreases, $\gamma\tau$ becomes smaller than the size of the nucleus and the absorption cross section tends towards the absorption cross section of the final resonances. This implies that ψ' suppression is stronger than J/ψ suppression because of the larger size of the ψ' . The difference between α_ψ and $\alpha_{\psi'}$ was predicted to appear for negative $x_{\rm F}$ values at a beam energy of 200 GeV. However, the recent results of E866 show that at 800 GeV, the deviation appears around $x_{\rm F} = 0.25$ where $\gamma \simeq 50$ and seems to indicate that the τ_g values are smaller than what expected in Ref. [24]. A recent discussion of E866 results can be found in Ref. [26].

4. *A–B* collisions

As described in Ref. [4], as far as nuclear absorption is concerned, A–B collisions should be described as a superposition of A–p and p–B suppressions
$$S^{AB}_{J/\psi}(x_{\rm F}; AE_p) = S^{Ap}_{J/\psi}(x_{\rm F}; AE_p) \cdot S^{pB}_{J/\psi}(x_{\rm F}; E_p)\,. \tag{4.1}$$
While p–B collisions are well studied, there no are results about inverse kinematics collisions A–p. By changing the reference system, one has
$$S^{Ap}_{J/\psi}(x_{\rm F}; AE_p) = S^{pA}_{J/\psi}(-x_{\rm F}; E_p)\,. \tag{4.2}$$

At 200 GeV, there exists no results for negative $x_{\rm F}$ values and the extrapolation from the positive region is not straightforward due to the formation time effects discussed above. For NA50 (and previously NA38), $\bar{x_{\rm F}}$=0.15 and the Lorentz γ factor changes from 16 to 6 when $x_{\rm F}$ changes from 0.15 to -0.15. In the establishment of the reference of "normal" suppression, this fact is usually not taken into account. The suppression factor is just taken as

$$S^{AB}_{J/\psi}(x_{\rm F}, E_{\rm T}; E_p) = {\rm e}^{-\sigma_{\rm abs}(J/\psi)\rho_0(L_A+L_B)}, \tag{4.3}$$

where the lengths L_A and L_B for the trajectories of the $c\bar{c}$ in the projectile and target are estimated from the geometry of the collision. The impact parameter b is deduced from a simulation of the $E_{\rm T}$ distribution [27]. The relation between b and L is then straightforward.

4.1. L-scaling

Both J/ψ cross sections and ψ/DY ratios have been plotted as a function of L. For instance, this is shown in Fig. 11 for the ψ/DY ratio. The advantage of the L variable is that it allows to put in the same figure different target-projectile systems and also different centrality bins in a given system.

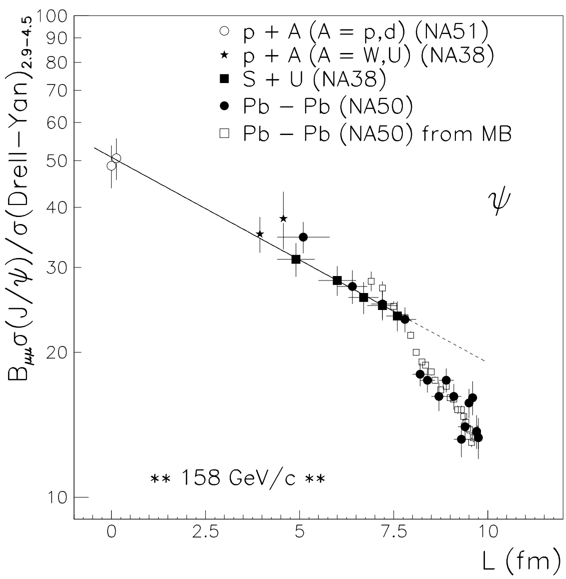

Fig. 11. J/ψ suppression pattern in different target-projectile systems versus the length of matter in the final state.

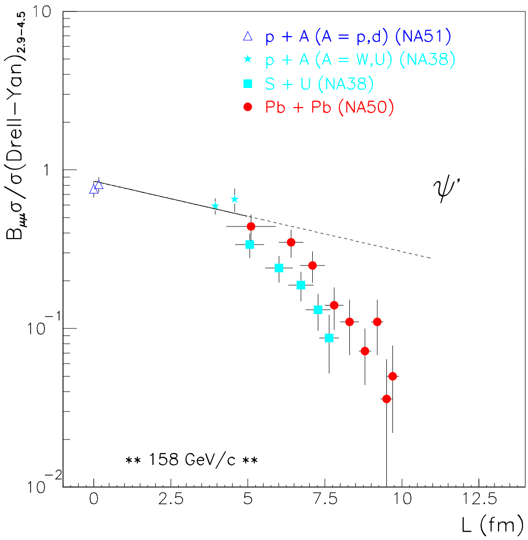

Fig. 12. The same as Fig. 11 for ψ'

Fig. 11 is equivalent to Fig. 7 but it also includes previous NA38 and NA51 p–A [10, 11] and S–U [28] results. The exponential fit does not include Pb–Pb data and leads to an absorption cross section $\sigma_{\text{abs}} = 6.3 \pm 1.0$ mb [3]. The dotted line in Fig. 7 is equivalent to the exponential line in Fig. 11. The Pb–Pb systems clearly shows the new features cited above: *i)* the suppression in peripheral collisions agrees with that measured in lighter systems, *ii)* above $L = 8$ fm, there is an additional suppression which is called "anomalous" by the NA50 collaboration. The new 1998 data, which show a second drop around $L = 9.3$ fm, are not yet included in the figure. Some comments can be made:

- The suppression increases very suddenly above $L = 8$ fm giving rise to a "step" behaviour and not only to a "break".
- There is a saturation of the L parameter for the most central collisions because of the geometry and L is not the best variable to describe the new physics.
- In a given system, L is roughly proportional to the energy density. This means that, for the second drop, the energy density is multiplied by about 1.16.

[3] The expression (4.3) is exact only if $\rho_0\sigma_{\text{abs}}(L_A + L_B) \ll 1$. The full calculation leads to a value $\sigma_{\text{abs}} = 7.3$ mb [29] instead of the effective value of 6.3 mb.

- In order to compare J/ψ behaviour to results obtained for other signatures of the QGP, it is interesting to know the number of participant nucleons corresponding to the two discontinuities. In the framework of the wounded nucleon model [30], $N_{\text{part}} \simeq 140$ for the first drop and $\simeq 320$ for the second one.

The ψ' suppression with Drell–Yan as a reference is shown in Fig. 12 [12]. Contrary to p–A collisions, ψ' suppression in Pb–Pb is stronger than J/ψ suppression. But it is also the case for S–U collisions. There is a factor about 20 between the suppression of ψ' in p–p collisions and its value for central Pb–Pb. It can be noted also that ψ' suppression is about 1.5 times less important in Pb–Pb than in S–U collisions at the same L value.

4.2. Is a QGP formed?

The new results of NA50, with two discontinuities in the suppression pattern, cannot be accounted for by conventional physics. They have been abundantly discussed in the framework of models based on QGP formation [1,31–36] which provide a natural way of introducing a threshold physics. Details about these calculations can be found in the review papers. Their main idea is the following: when the energy density (or the temperature) reaches the value required for the phase transition, then the J/ψ is completely suppressed, either by Debye screening or by gluon dissociation [32]. Below ε_{c}, it only suffers absorption in nuclear matter as described above. However, a sudden change in the J/ψ suppression is observed experimentally (for instance, see Fig. 11) which cannot be accounted for by the above picture: indeed, if the critical energy density is reached at a some impact parameter, then the size of the volume in which it happens increases smoothly with the centrality of the collision. In order to produce a step behaviour, a "discontinuity" hypothesis must be introduced. Different ideas have been proposed. In Ref. [34], it is assumed that apart from the temperature which must be above T_{c}, the volume must be also above a critical V_{c} value because it must be large enough to overcome the interface tension between the two phases. However, as mentioned in Ref. [36], this introduces a discontinuous change in the equation of state which leads to a jump in entropy. The experimental multiplicity of particles do not exhibit such a discontinuity.

Recently another idea has been proposed [35, 37]. The approach to the critical behaviour is described in the framework of the percolation model. The formation of clusters is studied in the finite size environment of the collision zone. The percolation behaviour of the strings formed between the collision partners [35] or equivalently of the partons [37] is studied when their density increases. It is shown that there is a strong variation of the cluster size around the percolation point while the density of clusters itself shows a smooth variation. The main parameter used in these calculations is the radius of the strings (or partons) which governs the abruptness of the break. Fig. 13 from Ref. [37] shows the results of the model.

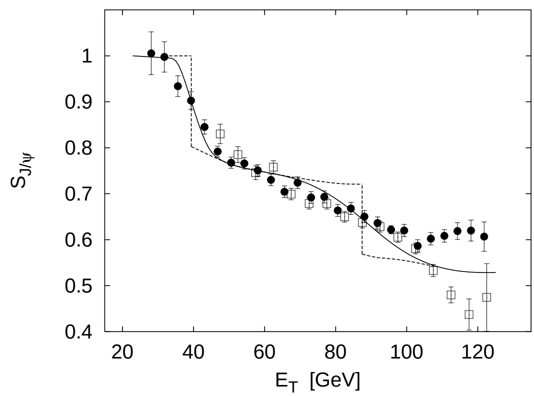

Fig. 13. J/ψ suppression pattern in the framework of the percolation model of Ref. [37]. The dashed line corresponds to a fixed $E_{\mathrm{T}} - b$ correlation while the solid line includes the $E_{\mathrm{T}} - b$ smearing.

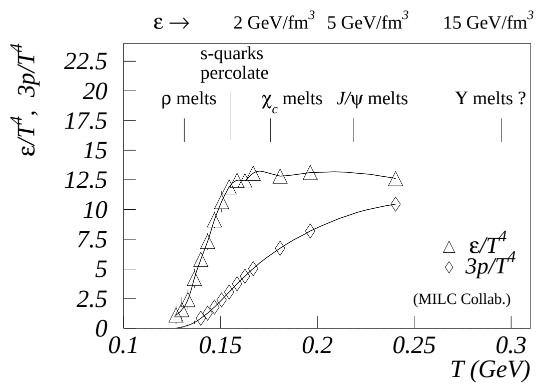

Fig. 14. Lattice-QCD equation of state and QGP signatures (from Ref. [38]).

Finally, a step appears naturally in Ref. [36] and is attributed to the non-trivial character of the equation of state at the phase transition.
In the framework of the QGP models, one must understand why there are two thresholds as observed in Fig. 9. This is usually related to the fact that 32 % of the measured J/ψ 's are fed from the decay of χ mesons and 8 % from the ψ'. It is easier to destroy the χ and the ψ' because they have larger radii and the first step is assumed to correspond to the χ meson suppression and the second one to the J/ψ itself (Fig. 13). However, if we deal with

a system in thermodynamical equilibrium, we should have $\varepsilon \propto T^4$. That means that if the χ is suppressed at the critical temperature, from what is said above *i.e.* $\varepsilon_\chi \simeq 1.16\ \varepsilon_\psi$, the J/ψ is suppressed at 1.04 T_c which is smaller than the QCD estimates (see for instance Fig. 14 from Ref. [38]).

4.3. Is the comover effect really negligible?

A lot of particles are produced in a heavy ion collisions and it has been considered that J/ψ or ψ' could be suppressed by destructive interactions with comoving particles in a further stage of the collision. There is a general consensus that ψ' which is a weakly bound state is very sensitive to such an effect.

As far as J/ψ is concerned, the subject has been much debated because of the lack of knowledge of the exact value of the cross section $\sigma_{\psi-\pi}$. In many calculations [39,40], it is considered as a free parameter at the same time as the nuclear absorption cross section of the premeson. But even when it is calculated, as pointed out at the Conference QM99 [41], the values differ by at least two orders of magnitude in the relevant energy range depending on the model [32,42,43] (Fig. 15).

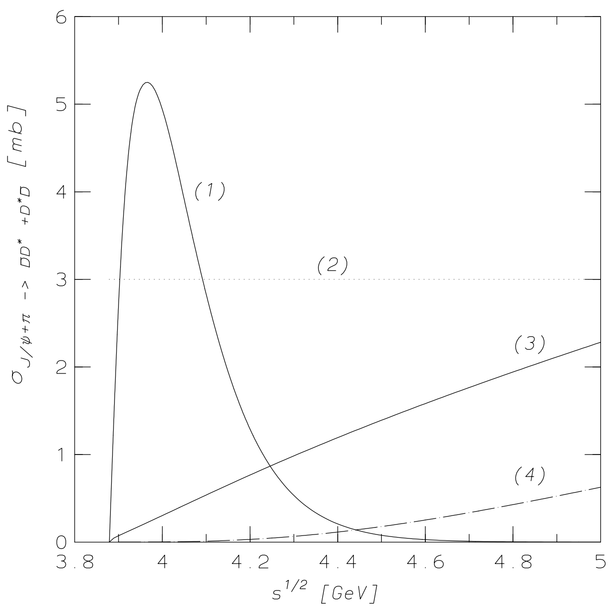

Fig. 15. Energy dependence of the J/ψ absorption cross section on pions following different models: (1) refers to the quark exchange model [42], (2) is an effective value, (3) is calculated with an effective hadronic Lagrangian [43] and (4) uses a short distance QCD approach [32]. The figure is from Ref. [41].

In any case, it is clear that such a conventional explanation cannot account for discontinuities in the suppression. And thus, while cross sections integrated over the impact parameter are rather well reproduced, the centrality dependence is not satisfactory at low E_{T} and always predicts a saturation of the suppression at high E_{T} values [44–50].

4.4. Other effects

Other effects have been considered and their description can be found in Ref. [4] but they can never account for the J/ψ centrality dependence in Pb–Pb.
Finally, in a detailed calculation [51,52], J/ψ is assumed to be suppressed by prompt gluons which are the debris from wounded nucleons. The interest of such a model is that most of the parameters are calculated instead of being simply extracted from a fit. As in the case of the comovers, the integrated cross sections are well reproduced but there are no discontinuities in the centrality dependence.

4.5. Does the J/ψ behave like a pion?

This unexpected question arose during the school in the lectures of M. Gazdzicki. I would like to bring here some partial answers.

4.5.1. Rapidity distribution of J/ψ

During the school, A. Capella made the objection that the x_{F} dependence of the α parameter is different for the J/ψ 's and the pions. In fact, it is even simpler to consider directly the rapidity distributions. It is well known that pion production, which is a soft process, has a rapidity distribution with its maximum value at the rapidity of the center of mass of the participant nucleons. In particular, it is increasingly shifted towards low rapidities when the mass of the target increases and the system becomes more asymmetric. This is not the case for the J/ψ . The rapidity distribution is always centered on the rapidity of the nucleon–nucleon collision as would be expected for a hard process. For instance, this has been checked by NA38 at 450 GeV [11] where dimuons are measured in the rapidity domain [-0.4, +0.6]. In order to determine the J/ψ acceptance, the rapidity distribution is fitted by a Gaussian distribution centered on y^*=0 and with $\sigma_{y^*} = 0.6$. Although the experimental rapidity domain is rather narrow, the results are very sensitive to the position of the maximum of the rapidity distribution and distributions shifted towards lower y values are not compatible with the data.

4.5.2. J/ψ multiplicity per participant nucleon

It has been stated by Gazdzicki (see lecture notes in this school and Ref. [53]) that the J/ψ behaved like a pion because the ratio $R_\psi = M_\psi/N_{\rm part}$ was constant with $N_{\rm part}$. M_ψ is the J/ψ multiplicity at a given impact parameter and $N_{\rm part}$ the corresponding number of participant nucleons. In a precise analysis, this is not true. In order to draw convincing conclusions, it is interesting to compare different target-projectile systems. The minimum bias spectrum which is needed to deduce the J/ψ multiplicity variation as a function of centrality has been measured by NA50 for Pb–Pb collisions only. However, there is an indirect way to deduce the ratio R_ψ from the measurement of $\sigma_\psi/\sigma_{\rm DY}$. Since $\sigma_{\rm DY}$ is proportional to the number of nucleon–nucleon collisions $N_{\rm coll}$, then R_ψ is proportional to $\sigma_\psi/\sigma_{\rm DY} \times N_{\rm coll}/N_{\rm part}$. In the following, $N_{\rm coll}$ and $N_{\rm part}$ are simulated using the wounded nucleon model [30]. The result is shown in Fig. 16 where the curve has been normalized to the value for pp collisions. Here $N_{\rm coll}/N_{\rm part}$=0.5 and $R_\psi(pp) = 2.14/N_{\rm part} \times \sigma_\psi(pp)/\sigma_{\rm inel}(pp) = 0.83\ 10^{-6}$ with $B\ \sigma_\psi^{\mu\mu}(pp) = 1.6$ nb at 158 GeV, $\sigma_{\rm inel}(pp) = 32$ mb and $N_{\rm part} = 2$.

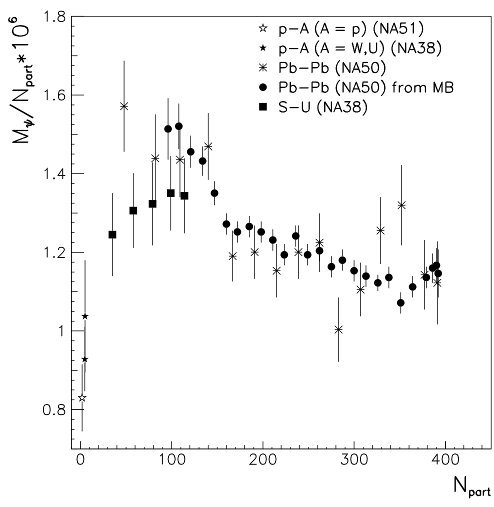

Fig. 16. J/ψ multiplicity per participant nucleon vs the number of participant nucleons.

The factor 2.14 is needed to extrapolate the NA50 phase space to the whole forward hemisphere. The negative $x_{\rm F}$ region is not considered because of the possible formation time effects described in section 3.2. Finally, B is the branching ratio of the decay of J/ψ into muon pairs, $B = 6\%$. Some comments about Fig. 16:

- The ratio is not constant between p–p and central Pb–Pb. The opposite conclusion could be drawn in Ref. [53] since only cross sections integrated over the impact parameter are considered. These cross sections are not very sensitive to the new physics which appears in the centrality dependence as is also observed for the interpretation of the J/ψ suppression in terms of the comover effect (Section 4.3). Moreover, absolute cross sections always have large systematic errors while the ratios do not.

- There is no scaling between p–p, p–A, S–U and peripheral Pb–Pb collisions because $N_{\rm part}$ is not the adequate parameter.

- The peculiar behaviour of the J/ψ suppression pattern per participant can be understood when looking at the "theoretical" behaviour of the Drell–Yan process. With Drell–Yan being proportional to the number of nucleon–nucleon collisions, the ratio $R_{\rm DY} = M_{\rm DY}/N_{\rm part}$ behaves like the ratio $N_{\rm coll}/N_{\rm part}$ which is shown in Fig. 17. $R_{\rm DY}$ is thus observed to increase by a factor 5 between p–p and central Pb–Pb collisions. If initial state effects such as shadowing are neglected, Fig. 17 represents also the production pattern of $c\bar{c}$ pairs. To this production mechanism, one must add a final state suppression mechanism. As long as the suppression is not too strong, R_ψ increases, as in S–U for instance. When the suppression increases further, there is a maximum and then R_ψ decreases again. For this reason the integrated value may appear quasi constant from S–U to Pb–Pb.

- In Fig. 16, the first drop observed in Pb–Pb collisions is clearly displayed. This figure has been obtained for the 1996 data and the second drop is not included.

- Of course the ratio R_ψ depends on the value of $N_{\rm coll}/N_{\rm part}$ which in turn depends on the determination of the impact parameter and one may wonder if the variations observed are not due to an incorrect estimation of b (or $N_{\rm part}$) from the $E_{\rm T}$ spectrum. Among the heavy ion community, there are on-going discussions about the best way of determining $N_{\rm part}$ but it can be seen from Fig. 17 that rather important changes of $N_{\rm part}$ are required in order to make flat the $N_{\rm part}$ dependence of the ratio [4].

[4] A side remark can be made about Fig. 17. It has been claimed that for the strangeness signature, there was a difference of strangeness enhancement between central S–S collisions and peripheral Pb–Pb collisions at $N_{\rm part} \simeq 50$ because the number of nucleon–nucleon collisions was different. It is clear that it is not the case and that another parameter is needed to adequately describe the available results concerning strangeness enhancement.

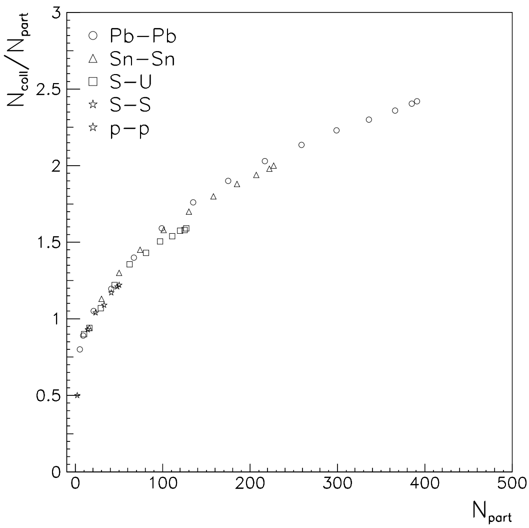

Fig. 17. Number of nucleon–nucleon collisions per participant nucleon vs the number of participant nucleons. This ratio represents also the theoretical behaviour of the Drell–Yan multiplicity per participant nucleon.

4.5.3. Is the production of ψ' statistical?

If there is a statistical production of J/ψ at hadronization, it should also be the case for ψ'. Using the ratio of the statistical yields of ψ' to J/ψ [53] and the hadronization temperature $T_{\rm H} = 170$ MeV extracted from [53] one gets

$$M_{\psi'}/M_{\psi} = (m_{\psi'}/m_{\psi})^{3/2}\ \exp(-(m_{\psi'} - m_{\psi})/T_{\rm H}) = 4\%, \qquad (4.4)$$

where m_{ψ} and $m_{\psi'}$ are the relative masses of the two mesons. Following the arguments of Ref. [53], the 4% value should be observed for all systems. This is not the case. This value is only reached for the most central Pb–Pb while it is $\simeq 13\%$ for p–A collisions.

From all these arguments, it appears that the J/ψ does not behave like a pion.

5. Conclusion

The J/ψ suppression pattern as measured by the NA50 collaboration in Pb–Pb collisions, and in particular the second threshold shown for the first time at QM99 Conference, cannot be trivially explained. The existence of the two thresholds is really essential and it should be searched for in other systems. For instance Sn–Pb collisions may help to study the first step in better conditions. Sn–Pb collisions are better than Pb–Sn in order to avoid the increasing importance of inverse kinematics where the hadronic reference is not well known. A symmetric system such as Sn–Sn should be more interesting but is expected to exhibit the first threshold at a too high E_{T} value and cannot lead to an unambiguous observation of the anomalous suppression. Pb–U (and even better U–U...) collisions should exhibit the second drop at a value of E_{T} below the knee in a region where the E_{T} distributions of both J/ψ and minimum bias distributions are flat and not sensitive to potential systematic effects related to the difference of triggers. In order to get a more precise description of the anomalous physics some questions should be answered:

- How to extrapolate the normal suppression to heavy systems? Can we neglect the contribution of the inverse kinematics part of the collision (Eq. 4.1)? The new results from E866 show that this is not trivial.
- Is the color octet model still valid at low p_{T}? What happens if the time for colour neutralisation is shorter?
- In the framework of the QGP explanation, why is the temperature for J/ψ dissolution only 1.04 times that for the χ?
- How can the J/ψ suppression pattern be related to other signatures and in particular to strangeness which is claimed to saturate as of a very low value of about 50 participants where the J/ψ and ψ' suppressions are "normal"?
- Is it possible to get a reliable calculation of the comover effective cross section in a hadronic gas of imprecisely known composition?

All these questions should be answered before any definite conclusion can be drawn. But, in any case, the present results of NA50 are difficult to understand with conventional physics only.

The author wants to thank N. Willis and M. MacCormick for their comments on the manuscript.

REFERENCES

[1] T. Matsui, H. Satz, *Phys. Lett.* **B178**, 416 (1986).
[2] B. Mueller, nucl-th/9806023 (1998).
[3] R. Vogt, *Phys. Rep.* **310**, 197 (1999).
[4] C. Gerschel, J. Huefner, *Annu. Rev. Nucl. Part. Sci.* (1999) to be published.
[5] M.C. Abreu *et al.* (NA50 Collaboration), *Phys. Lett.* **B410**, 327 (1997).

[6] M.C. Abreu *et al.* (NA50 Collaboration), *Phys. Lett.* **B450**, 456 (1999).
[7] F. Bellaiche *et al.* , *Nucl. Instrum. Methods. Phys. Res. Sect. A* **398**, 180 (1997).
[8] C. Cicalo *et al.* (NA50 Collaboration), Quark Matter 99 Conference, Torino, Italy, (1999).
[9] R. Arnaldi *et al.* , *Nucl. Instrum. Methods. Phys. Res. Sect. A* **411**, 1 (1998).
[10] A. Baldit *et al.* (NA51 Collaboration), *Phys. Lett.* **B332**, 244 (1994).
[11] M.C. Abreu *et al.* (NA38 Collaboration), *Phys. Lett.* **B444**, 516 (1994).
[12] L. Ramello *et al.* (NA50 Collaboration), Quark Matter 97 Conference, Tsukuba, Japan (1997).
[13] C. Gerschel, J. Huefner, *Z. Phys.* **C56**, 171 (1992).
[14] J. Badier *et al.* (NA3 Collaboration), *Z. Phys.* **C20**, 101 (1983).
[15] C. Baglin *et al.* (NA38 Collaboration), *Phys. Lett.* **B270**, 105 (1991).
[16] D.M. Alde *et al.* (E772 Collaboration), *Phys. Rev. Lett.* **66**, 133 (1991).
[17] M.J. Leitch *et al.* (E789 collaboration), *Phys. Rev.* **D52**, 4251 (1995).
[18] M.J. Leitch *et al.* (E766 collaboration), Quark Matter 99 Conference, Torino, Italy (1999).
[19] A.G. Clark *et al.* (E722 Collaboration), *Nucl. Phys.* **B142**, 29 (1978); L. Antoniazzi *et al.* (E705 Collaboration), *Phys. Rev.* **D46**, 4826 (1992); H.D. Snyder *et al.* (E444 Collaboration), *Phys. Rev. Lett.* **42**, 944 (1979).
[20] J. Hüfner, M. Simbel, *Phys. Lett.* **B258**, 465 (1991).
[21] J. Hüfner, B.Z. Kopeliovich, *Phys. Rev. Lett.* **76**, 192 (1996).
[22] G.T. Bodwin *et al.* , *Phys. Rev.* **D46**, 3703 (1992).
[23] G.T. Bodwin *et al.* , *Phys. Rev.* **D51**, 1125 (1995).
[24] D. Kharzeev, H. Satz, *Phys. Lett.* **B366**, 316 (1996).
[25] D. Kharzeev, H. Satz, *Phys. Lett.* **B356**, 365 (1995).
[26] Y.B. He *et al.* , hep-ph/9908243.
[27] M.C. Abreu *et al.* (NA50 Collaboration), *Phys. Lett.* **B410**, 337 (1997).
[28] C. Baglin *et al.* (NA38 Collaboration), *Phys. Lett.* **B449**, 128 (1999).
[29] D. Kharzeev *et al.* , *Z. Phys.* **C** 74, 307 (1997).
[30] A. Bialas *et al.* , *Nucl. Phys.* **B111**, 461 (1976).
[31] F. Karsch, R. Petronzio, *Phys. Lett.***193**, 105 (1987); *Z. Phys.* **C37**, 627 (1988).
[32] D. Kharzeev, H. Satz, *Phys. Lett.* **B334**, 155 (1994).
[33] J.P. Blaizot, J.Y. Ollitrault, *Phys. Rev. Lett.* **77**, 1703 (1997).
[34] D. Kharzeev *et al.* , hep-ph/9707308 (1997).
[35] M. Nardi, H. Satz, *Phys. Lett.* **B442**, 14 (1998).
[36] E. Shuryak, D. Teaney, *Phys. Lett.* **B430**, 37 (1998).
[37] H. Satz, QM99 Conference, Torino, Italy (1999); hep-ph/9908339.

[38] B. Mueller, QM99 Conference, Torino, Italy (1999); hep-ph/99

[39] S. Gavin, R. Vogt, *Phys. Rev. Lett.* **78**, 1006 (1997).

[40] A. Capella *et al.* , *Phys. Lett.* **B393**, 431 (1997).

[41] P. Braun-Munzinger, K. Redlich, QM99 Conference, Torino, Italy (1999); nucl-th/9908026.

[42] K. Martins *et al.* , *Phys. Rev.* **D51**, 2723 (1995).

[43] S. G. Matinyan, B. Mueller, nucl-th/9806027.

[44] A. Capella *et al.* , *Phys. Rev.* **C59**, 395 (1999).

[45] W. Cassing, C.M. Ko, *Phys. Lett.* **B396**, 39 (1997).

[46] W. Cassing, E.L. Bratkovskaya, *Nucl. Phys.* **A623**, 570 (1997).

[47] C-Y. Wong, *Phys. Rev. Lett.* **76**, 196 (1996).

[48] D. Kahana, S. Kahana, *Phys. Rev.* **C59**, 1651 (1999).

[49] C. Spieles *et al.* , *Phys. Rev.* **C60**, 054901 (1999).

[50] J. Geiss, *et al.* , nucl-th/9810059.

[51] J. Huefner, B.Z. Kopeliovich, *Phys. Lett.* **B445**, 223 (1998).

[52] J. Huefner *et al.* , hep-ph/9908244.

[53] M. Gazdzicki, M.I. Gorenstein, *Phys. Rev. Lett.* **83**, 4009 (1999); hep-ph/9905515.